bioRxiv preprint doi: https://doi.org/10.1101/767830; this version posted September 26, 2019. The copyright holder for this preprint (which was not certified by peer review) is the author/funder. All rights reserved. No reuse allowed without permission.

Real-time dynamics of *Plasmodium* NDC80 as a marker for the kinetochore during atypical mitosis and meiosis

Rajan Pandey[1], Mohammad Zeeshan[1], David J.P. Ferguson[2,3], Robert Markus[1], Declan Brady[1], Emilie Daniel[1], Rebecca R. Stanway[4], Anthony A. Holder[5], David S. Guttery[6] and Rita Tewari[1*]

[1]School of Life Sciences, Queens Medical Centre, University of Nottingham, Nottingham, NG7 2UH; [2]Nuffield Department of Clinical Laboratory Science, University of Oxford, John Radcliffe Hospital, Oxford OX3 9DU, UK; [3]Department of Biological and Medical Sciences, Faculty of Health and Life Science, Oxford Brookes University, Gipsy Lane, Oxford OX3 0BP, U; [4]Institute of Cell Biology, University of Bern, Bern 3012, Switzerland, [5]Malaria Parasitology Laboratory, The Francis Crick Institute, London, NW1 1AT, UK; [6]Leicester Cancer Research Centre, University of Leicester, Leicester, LE2 7LX, UK.

These authors contributed equally: Rajan Pandey, Mohammad Zeeshan

[*]For correspondence

Rita Tewari: rita.tewari@nottingham.ac.uk

Short title: Expression and localization of Ndc80 in *Plasmodium*

bioRxiv preprint doi: https://doi.org/10.1101/767830; this version posted September 26, 2019. The copyright holder for this preprint (which was not certified by peer review) is the author/funder. All rights reserved. No reuse allowed without permission.

Abstract

Eukaryotic cell proliferation requires chromosome replication and precise segregation, followed by cell division, to ensure daughter cells have identical genomic copies. The kinetochore is a multi-protein structure assembled on chromosome centromeres, which mediates attachment to spindle microtubules and chromosome segregation during mitosis. *Plasmodium* spp*.,* the causative agent of malaria, undergoes closed mitosis with an intact nuclear membrane and intranuclear mitotic spindle. However, the regulation of the main events of mitosis and meiosis, including chromosome segregation, is poorly understood in this parasite. In part this is due to a distinct lack of markers for tracking kinetochore dynamics. Since NDC80 is the conserved component of the kinetochore complex, we labelled NDC80 with either a C-terminal GFP or mCherry tag by recombination at the endogenous locus to generate transgenic lines of the rodent malaria parasite *Plasmodium berghei*. We show that NDC80 is located at a single cluster of all kinetochores and examine its spatio-temporal dynamics throughout all proliferative stages of the parasite life cycle. We also compare the location of NDC80 with that of the kinetochore using electron microscopy. These transgenic parasite lines are a very useful resource to identify and study the kinetochore complex and follow chromosome dynamics during malaria parasite development.

Keywords:

Malaria, *Plasmodium*, kinetochore, NCD80, atypical cell division, endomitosis, meiosis.

Summary Statement

The dynamic localization of NDC80, a kinetochore marker, is examined throughout the proliferative stages of malaria parasite life-cycle which provides a useful resource to study kinetochore complexes and chromosome dynamics.

bioRxiv preprint doi: https://doi.org/10.1101/767830; this version posted September 26, 2019. The copyright holder for this preprint (which was not certified by peer review) is the author/funder. All rights reserved. No reuse allowed without permission.

Introduction

Mitosis and meiosis are fundamental processes in cell division that enable DNA replication and chromosome segregation, and allow eukaryotic organisms to proliferate, propagate and survive (Cheeseman, 2014; McKinley and Cheeseman, 2016; Musacchio and Desai, 2017; Vader and Musacchio, 2017). During these processes, microtubular spindles form to facilitate an equal segregation of duplicated chromosomes to the spindle poles. Chromosome attachment to the spindle microtubules (MTs) is mediated by kinetochores, which are large multi-protein complexes assembled on the centromere located at the constriction point of sister chromatids. Each sister chromatid has its own kinetochore, oriented to facilitate movement to opposite poles of the spindle apparatus. During anaphase, the spindle elongates and the sister chromatids separate, resulting in segregation of the two genomes during telophase. A key component of the kinetochore that mediates its attachment to spindle MTs is the NDC80 complex. The NDC80 complex is a key component of the network of conserved Knl1, Mis12 and Ndc80 complexes (KMN) (McKinley and Cheeseman, 2016; Petrovic et al., 2016). The ~170-190 kDa NDC80 complex has two globular domains at either end of a ~57 nm elongated coiled-coil, forming a dumb-bell shape. It is a heterotetramer comprising a 1:1:1:1 ratio of NDC80 (also known as HEC1 in humans), NUF2, SPC24 and SPC25 sub-complexed as two heterodimers: NDC80 with NUF2 and SPC24 with SPC25 (Ciferri et al., 2005; Farrell and Gubbels, 2014; Wei et al., 2005). The C-termini of the SPC24-SPC25 dimer anchor the complex to the kinetochore; whereas the NDC80-NUF2 dimer mediates plus-end MT binding through its calponin homology domain (CHD) (Alushin et al., 2010; Farrell and Gubbels, 2014; Sundin et al., 2011).

Malaria, caused by the apicomplexan parasite *Plasmodium* spp., remains one of the most prevalent and deadly infectious diseases worldwide, with 219 million clinical cases and 435,000 deaths in 2017 (WHO, 2018). *Plasmodium* has several morphologically distinct proliferative stages during its life cycle that alternates between vertebrate host and mosquito vector (**Fig.1**) (Francia and Striepen, 2014; Sinden, 1991a; Sinden, 1991b). A malaria parasite-infected female anopheles mosquito inoculates haploid sporozoites into the mammalian host during a blood meal. Sporozoites travel through blood stream to the liver and infect hepatocytes, where the parasite replicates and develops and into a schizont. At the end of this exo-erythrocytic schizogony the host cell is ruptured to release haploid merozoites, which infect erythrocytes. In the intra-erythrocytic phase, an initial ring stage form develops through the trophozoite form into a schizont, where multiple rounds of asexual multiplication occurs (erythrocytic schizogony). At the end of schizogony, host cell rupture releases further merozoites that infect new erythrocytes.

bioRxiv preprint doi: https://doi.org/10.1101/767830; this version posted September 26, 2019. The copyright holder for this preprint (which was not certified by peer review) is the author/funder. All rights reserved. No reuse allowed without permission.

Following erythrocyte invasion, some parasites differentiate into male (micro) and female (macro) gametocytes to initiate the sexual phase of the life cycle, which occurs in the mosquito. These haploid parasites are arrested at the G0/G1 phase of the cell cycle (Arnot and Gull, 1998). Following activation by mosquito ingestion, gametogenesis is initiated. Male gametogenesis is very rapid and within 15 min after activation eight motile microgametes are released. Gametogenesis can be studied *in vitro* using a medium that mimics the mosquito midgut environment (Tewari et al., 2005).

After fertilisation the zygote differentiates into a motile ookinete. The ookinete invades the mosquito midgut wall where it develops into an oocyst. At this stage multiple rounds of endomitotic division occurs in a process is similar to what is observed during schizogony, which is followed by cytokinesis to form thousands of motile sporozoites (Francia and Striepen, 2014; Gerald et al., 2011). The sporozoites are released from the oocyst and migrate to the mosquito's salivary glands for transmission to the vertebrate host.

The life cycle of *Plasmodium* is characterized by two unique processes of mitosis and a single stage of meiosis. The first mitotic process occurs during schizogony within mammalian hepatocytes and erythrocytes, and during sporogony in oocysts in the mosquito vector (Sinden, 1991a; Sinden, 1991b) (**Fig. 1 (A)**). This mitotic division is atypical, for example no clear G2 cell cycle phase has been observed during schizogony (Arnot and Gull, 1998; Doerig et al., 2000). This asexual proliferation is characterised by multiple rounds of asynchronous nuclear division without chromosome condensation and in the absence of cytokinesis. Mitosis is closed, occurring without dissolution and reformation of the nuclear envelope, and the spindle-pole body/microtubule-organising centre (MTOC), also known as the centriolar plaque (Arnot et al., 2011; Francia et al., 2015; Sinden, 1991b), is embedded within the nuclear membrane. The asynchronous nuclear division precedes cell division, leading to a multinucleate syncytium. The last round of nuclear division in these cells is synchronous and it is only after this final round of mitosis that cytokinesis occurs to form the haploid daughter merozoites or sporozoites, respectively. The second type of mitotic division occurs during male gametogenesis (**Fig. 1 (B)**), following activation in the mosquito midgut. Three rounds of rapid genome duplication (from haploid to octoploid) without concomitant nuclear division (endoreduplication) are followed by chromosome condensation and nuclear budding into the flagellated male gamete during exflagellation within 12 to 15 min after activation (Arnot and Gull, 1998; Janse et al., 1988; Sinden, 1983). The resultant eight flagellated microgametes, each contain a haploid genome (Guttery et al., 2015; Sinden et al., 2010). Fertilization of the female gamete results in a diploid zygote, which develops and differentiates over a 24-hour period into a motile ookinete in the mosquito gut (**Fig. 1 (C)**). It is in this stage that meiosis

bioRxiv preprint doi: https://doi.org/10.1101/767830; this version posted September 26, 2019. The copyright holder for this preprint (which was not certified by peer review) is the author/funder. All rights reserved. No reuse allowed without permission.

occurs. The DNA is duplicated once to form a tetraploid cell and then two rounds of chromosome segregation result in four discrete haploid genomes prior to ookinete maturity. Reductive division to haploidy presumably occurs in the subsequent oocyst during sporozoite formation (Guttery et al., 2015; Sinden, 1991a; Sinden, 1991b). These different stages of cell division and proliferation indicate that the parasite has evolved alternate modes of chromosome replication, condensation and segregation, and nuclear and cell division at different stages in the life cycle.

The process of chromosome segregation and kinetochore dynamics throughout the life cycle are not well understood. To date, analysis of *Plasmodium* mitotic/meiotic spindle assembly and chromosome segregation has been performed largely using transmission electron microscopy (TEM) (Sinden et al., 1978; Sinden et al., 1976), and biochemical analysis of microtubule markers including α-tubulin (Fennell et al., 2008), and centrins associated with the putative MTOC (Gerald et al., 2011; Roques et al., 2019). An analysis of a *Plasmodium* artificial chromosome (PAC) identified a putative centrosome derived from chromosome 5 (*PbCEN5*), and highlighted the dynamics of chromosome segregation during both mitotic and meiotic stages of the parasite's life cycle (Iwanaga et al., 2010). To complement these studies, we have analysed the real time expression and spatiotemporal dynamics of NDC80, as a kinetochore marker. We generated a stable transgenic *P. berghei* line expressing NDC80 with a C-terminal GFP-tag by modifying the endogenous locus, and examined NDC80 location during mitosis in schizogony, sporogony and male gametogenesis, and during meiosis in ookinete development. We used fluorescence microscopy in real time with live cells, and co-localisation immunofluorescence studies with fixed cells. We complemented these fluorescence microscopy studies with ultrastructural studies using electron microscopy. We observed kinetochores of all chromosomes as clustered yet distinct NDC80-GFP foci adjacent to the nuclear DNA during each stage, with the number of foci corresponding to the likely ploidy of individual nuclei. This transgenic parasite line expressing NDC80-GFP is a valuable resource for studying chromosome segregation and dynamics, as well as identifying the various protein complexes involved in these processes during cell division in the malaria parasite.

bioRxiv preprint doi: https://doi.org/10.1101/767830; this version posted September 26, 2019. The copyright holder for this preprint (which was not certified by peer review) is the author/funder. All rights reserved. No reuse allowed without permission.

Results

Real-time live cell imaging using NDC80-GFP reveals kinetochores aggregated as discrete foci during schizogony.

To study kinetochore dynamics, we generated NDC80-GFP, a transgenic *P. berghei* line expressing NDC80 with a C-terminal GFP tag, by inserting the *gfp* coding sequence at the 3' end of the endogenous *ndc80* locus using single homologous recombination (**Fig. S1A**). We also generated a NDC80-mCherry line using the same strategy (**Fig. S1A**). Successful insertion was confirmed by PCR (**Fig. S1B**). Western blot analysis of a schizont protein extract using an anti-GFP antibody revealed the NDC80-GFP protein at the expected size of 96 kDa compared to the size of GFP alone at 29 kDa (**Fig. S1C**).

Following successful generation of the NDC80-GFP transgenic line, the spatiotemporal profile of NDC80-GFP protein expression and location was examined during the parasite life cycle at the three asexual mitotic replicative stages (liver and blood schizogony in the vertebrate host and oocyst development (sporogony) in the mosquito vector (**Fig. 1A**), the sexual mitotic stage (male gametogenesis) (**Fig. 1B**) and the meiotic stage (ookinete development) (**Fig. 1C**).

In the asexual blood stage, no fluorescence was observed in the intra-erythrocytic ring stage, a non-replicative G1 phase of the cell cycle, when RNA and protein synthesis first begins (Arnot and Gull, 1998; Doerig et al., 2000) (**Fig. 2A**). A faint but discrete single focus of NDC80-GFP adjacent to the nuclear DNA was observed in the early trophozoite, which became more intense as the trophozoite developed (**Fig. 2A**). The late trophozoite stage marks the transition into early S phase of the cell cycle, when DNA synthesis starts; however, prior to DNA synthesis trophozoites have high levels of pre-accumulated RNA (Arnot and Gull, 1998; Doerig et al., 2000). Onset of schizogony is the start of nuclear division and was marked by duplication of the NDC80-GFP into two foci lying in close proximity to each copy of nuclear DNA, revealing that DNA replication and sister chromatid separation had occurred, as marked by the two kinetochore foci and followed by nuclear division. Similar fluorescence patterns were also observed in the NDC80-mCherry line (**Fig. S2**). We also observed asynchronous nuclear division during early schizogony, as marked by two or more nuclei with both single and double distinct NDC80 foci adjacent to single DNA masses (**Fig. 2A**). As alternating repeated S/M phases, following the division of individual nuclei continued, these NDC80-GFP foci were duplicated several times into multiple foci. Further in-depth analysis of NDC80-GFP localization by super resolution microscopy confirmed the asynchronicity of nuclear division during blood stage schizogony as shown in **Fig. 2B and Supplementary video SV1, SV2 and SV 3.** This stage of DNA replication and nuclear division is terminated by the cytokinesis

bioRxiv preprint doi: https://doi.org/10.1101/767830; this version posted September 26, 2019. The copyright holder for this preprint (which was not certified by peer review) is the author/funder. All rights reserved. No reuse allowed without permission.

that only occurs at the end of the nuclear division phase (Arnot and Gull, 1998; Doerig et al., 2000). Although the discrete NDC80-GFP foci were present in late schizonts and developing merozoites, they had disappeared from mature merozoites. The short-lived, extracellular merozoite represents part of the G1 phase of the cell cycle (Arnot and Gull, 1998; Doerig et al., 2000). During schizogony in the pre-erythrocytic asexual stage in the liver, discrete fluorescent foci next to nuclear DNA were observed, which is similar to the pattern in blood stage schizogony (**Fig. S3**).

To complement the live-imaging analysis, erythrocytic schizogony was examined in ultrastructural studies. In the multinucleated schizont during merozoite formation, it was possible to identify nuclear poles with radiating microtubules and attached kinetochores at just one side of the nucleus **(Fig. 2C)**. However, these structures were not visible in the mature merozoite or early intracellular ring stage. These observations are consistent with the live-imaging data.

Immunofluorescence imaging shows NDC80-GFP does not co-localize with centrin and α-tubulin

To determine whether NDC80-GFP is located at the spindle and/or centrosome, we used immunofluorescence-based co-localization assays with anti-GFP antibodies and anti-α-tubulin and anti-centrin, as markers for the spindle and centrosome (spindle pole body), respectively. We observed that NDC80-GFP is located adjacent to alpha-tubulin but there was no overlap between the two signals in schizonts (**Fig. 2D).** This indicates that NDC80-GFP does not co-localize with the spindle. Similarly, using anti-GFP with anti-centrin antibodies revealed that NDC80-GFP is located in close proximity to, but does not co-localize with centrin (**Fig. 2E**). These observations suggest that NDC80 is not part of the spindle or spindle pole body, but part of another structure likely to be the kinetochore.

Rapid spindle dynamics and NDC80-GFP localisation during endo-reduplication in male gamete development

We investigated the live cell dynamics of NDC80-GFP expression and location throughout the 15 min of male gametogenesis following gamete activation in vitro. The results are presented in **Fig. 3A**, together with a schematic guide (**Fig. 3A**) and time-lapse screenshots (**Fig. 3B and C, Supplementary videos SV4 and SV5.**). A single, rather diffuse and faint NDC80-GFP focus was present in non-activated male gametocytes, which intensified to a sharp single focal point within 1 min post-activation (mpa) (**Fig. 3A**). By 2 mpa, this focal point extended to form a bridge across one side of the nucleus, followed by the complete separation of the two halves

bioRxiv preprint doi: https://doi.org/10.1101/767830; this version posted September 26, 2019. The copyright holder for this preprint (which was not certified by peer review) is the author/funder. All rights reserved. No reuse allowed without permission.

of the bridge to produce two clear single foci by 3 mpa (**Fig. 3A-C)**. This process repeated twice, although non-synchronously, resulting in 8 discrete NDC80-GFP foci (**Fig. 3A**).

The ultrastructural analysis of the nucleus during microgametogenesis within 8 mpa showed typical nuclear spindles with microtubules radiating from the nuclear poles, to which attached kinetochores could be identified (**Fig. 3D**). The spindles with attached kinetochores were located on the inner side of the nuclear membrane, (**Fig. 3D**). It appears that two hemispindles associated with the kinetochore are joined together to form a mitotic spindle at the earliest stages. This is then followed by kinetochore movement to opposite poles once all the duplicated chromosomes are segregated. The mitotic process of duplication proceeds in the absence of nuclear division (karyokinesis), which is very atypical kinetochore dynamics but consistent with the live cell imaging data and further substantiating the analysis of NDC80-GFP real time dynamics.

The eight discrete foci associated with endoreduplication disappeared rapidly and no NDC80-GFP fluorescence was observed in flagellated motile microgametes following exflagellation (**Fig. S4**). Furthermore, no NDC80-GFP fluorescence was observed in either non-activated or activated female gametocytes (**Fig. S4**).

The spatiotemporal profile of NDC80-GFP expression in the meiotic stages during zygote differentiation to ookinete.

Meiosis in the malaria parasite occurs during zygote differentiation to the ookinete. This process takes 24 h to complete and during this time the ploidy of the parasite increases from 2N to 4N. To examine NDC80-GFP expression and kinetochore localisation throughout this process, we investigated the spatiotemporal profile of NDC80-GFP during ookinete differentiation.

NDC80-GFP fluorescence was first observed 1 to 1.5 h post-fertilization, during zygote to ookinete differentiation, as a single faint but distinct focal point, which gradually increased in intensity over the period 2 to 3 h post-fertilization (**Fig. 4**). As in microgametogenesis, the NDC80-GFP focus enlarged to form an elongated bridge-like feature, with multiple foci evident during stages II to IV of ookinete development, resulting in 4 discrete foci in the mature ookinete 18 h post-fertilization (**Fig.4A**). The ultrastructure of the mature ookinete clearly showed 4 kinetochores within an intact nuclear membrane, consistent with our live cell imaging (**Fig. 4B**).

bioRxiv preprint doi: https://doi.org/10.1101/767830; this version posted September 26, 2019. The copyright holder for this preprint (which was not certified by peer review) is the author/funder. All rights reserved. No reuse allowed without permission.

NDC80-GFP is present as multiple foci during oocyst development and sporozoite formation

During oocyst development and sporozoite formation, live cell imaging revealed NDC80-GFP fluorescence at multiple foci adjacent to the nuclear DNA during various stages of oocyst development from 7 days post-infection (dpi) of the mosquito to 21 dpi, as well as in mature sporozoites (**Fig. 5A and B**). Ultrastructure analysis of oocyst development revealed an enlarged nucleus that formed a large multiple lobed structure with multiple nuclear poles, followed by formation of large numbers of sporozoites at the plasmalemma of the oocyst (**Fig. 5Bi**), as described previously (Ferguson et al., 2014; Schrevel et al., 1977). Detailed examination showed nuclear poles with kinetochores directed toward the developing sporozoites (**Fig. 5Bii**). The endomitotic process of sporozoite formation during sporogony resembles that of merozoite formation within host red cells and hence is similar to schizogony.

Discussion

Cellular proliferation in eukaryotes requires chromosome replication and precise segregation, followed by cell division, to ensure that daughter cells have identical copies of the genome. This happens through assembly of a spindle to which the centromeric region of chromosomes are attached through the kinetochore. Kinetochores are specialized protein structures that assemble on centromeric regions of chromosomes to facilitate accurate chromosome segregation during cell division. Although the organisation of spindle microtubules and the modes of spindle pole separation vary (Akiyoshi and Gull, 2013; Drechsler and McAinsh, 2012), some kinetochore complex proteins like NDC80 are conserved across most eukaryotes, including Apicomplexan organisms (Akiyoshi and Gull, 2013). In higher eukaryotes, the kinetochore is well characterized and shown to have a trilaminar structure, with inner, middle and outer domains (Biggins and Walczak, 2003). The outer kinetochore domain contains the NDC80/NUF2 complex along with other MT-binding proteins, playing an important role in regulation of the stable attachment of the chromosomes to the MT spindle (DeLuca et al., 2002; Sundin et al., 2011). The structure and components of apicomplexan kinetochores have not been well characterized but NDC80 and NUF2 are present in *Toxoplasma* (Farrell and Gubbels, 2014).

In this study we have tried to unravel the expression, location and dynamics of NDC80 in *Plasmodium* by generating a transgenic parasite line to express GFP-labelled NDC80, a protein which faithfully replicates kinetochore location and function during all developmental stages of the life cycle. Live-cell imaging of the fluorescent protein, complemented with ultrastructural studies by electron microscopy, revealed a subcellular location of NDC80-GFP

bioRxiv preprint doi: https://doi.org/10.1101/767830; this version posted September 26, 2019. The copyright holder for this preprint (which was not certified by peer review) is the author/funder. All rights reserved. No reuse allowed without permission.

at discrete foci adjacent to nuclear DNA in all replicative stages of the *P. berghei* life cycle. The distribution and dynamic spatiotemporal profile corresponded to the replication of chromosomes during the atypical mitotic and meiotic processes of DNA replication in this organism. Non-replicating stages, including the intraerythrocytic ring stage, the extracellular mature merozoite, the non-activated female gametocyte and the motile male gametes show no evidence of NDC80-GFP expression. Overall, our results suggest that NDC80-GFP is an excellent marker for kinetochore dynamics during the replicative stages, and this will facilitate further comparative studies of chromosome replication and segregation in *Plasmodium.*

The subcellular localization data for NDC80-GFP revealed a discreet single focus adjacent to the haploid nuclear genome, which presumably contains the centromeres of all 14 chromosomes. Such clustering of centromeric regions has been demonstrated in yeast (Richmond et al., 2013), human cells (Solovei et al., 2004) and *Toxoplasma* (Farrell and Gubbels, 2014). It is thought to be important for genome integrity, but the exact reason for it is not well understood. In the stages of the life cycle where this NDC80 clustering is not detected, perhaps the 14 chromosomal centromeres are not clustered and therefore NDC80GFP expression is not detectable (Hoeijmakers et al., 2012). This is consistent with the idea that clustering of centromeres in *P. falciparum* occurs only prior to the onset of chromosomal division (Hoeijmakers et al., 2012). It is of interest that following fertilization there is a single focus despite the genome being diploid, perhaps this reflects the tight pairing of sister chromatids allowing recombination to occur at this stage.

Although our data showed a clustered location of NDC80, its actual role in chromosome clustering is not known. Previous studies on yeast and *Toxoplasma* showed no role of NDC80 in clustering, and suggested a sole role in attachment to spindle MTs during chromosome segregation. A single MT binds each kinetochore in budding yeast (Westermann et al., 2007); whereas in *Toxoplasma* a maximum of only 11 MTs were detected despite the fact that there are 14 chromosomes (Farrell and Gubbels, 2014; Swedlow et al., 2002). Within the closely related Coccidian parasites, a number of variations in the details of the process of asexual division have been described, relating to timing and number of genome and nuclear divisions (Ferguson et al., 2008) The coccidian parasite *Sarcocystis neurona*, which divides by Sarcocystis endopolygeny forms a polyploid nucleus culminating in 64 haploid daughter cells (Farrell and Gubbels, 2014; Vaishnava et al., 2005). During this process, intranuclear spindle poles are retained throughout the cell cycle, which suggests constant attachment of chromosomes to spindle MTs through kinetochores to ensure genome integrity throughout *Sarcocystis* cell division (Farrell and Gubbels, 2014; Vaishnava et al., 2005). In contrast, *Plasmodium* (a hemosporidian), undergoes classical schizogony with a variable number of

bioRxiv preprint doi: https://doi.org/10.1101/767830; this version posted September 26, 2019. The copyright holder for this preprint (which was not certified by peer review) is the author/funder. All rights reserved. No reuse allowed without permission.

cycles of genome replication and nuclear division resulting a multinucleated cell (Arnot et al., 2011). This is similar to what is seen in the coccidian parasites *Eimeria* spp and *Toxoplasma,* with daughter cell formation being associated with the final nuclear division. This fact is well demonstrated by the NDC80 localization in this study, which shows 1 or 2 NDC80-GFP foci per nucleus. The asynchronous nature of the division during these stages is shown by nuclei having both one and two NDC80GFP foci (and intermediate forms) within the same cell. We made similar observations in our previous study of CEN-4 (Roques et al., 2019). These studies also suggest that the kinetochore and centrosome/spindle pole body duplicate before nuclear division starts; therefore the duplication of NDC80 and CEN-4 sets the stage for mitosis at each round of nuclear division in *Plasmodium,* as in *Toxoplasma* (Suvorova et al., 2015). In contrast, during male gametogenesis the genome size increases to 8N, as clearly represented by 8 distinct NDC80-GFP foci, before nuclear division, although even in this case the chromosome replication and division is asynchronous. Similarly, during meiosis in ookinete development the genome size increases to 4N, represented by four distinct NDC80-GFP foci suggesting kinetochore clustering to facilitate chromosome segregation although no nuclear division takes place.

During sporogony multiple lobes are formed and the intranuclear spindle may be formed during multiple nuclear divisions as revealed by ultrastructural studies during sporozoite formation (Schrevel et al., 1977). Further ultrastructure analyses describe typical nuclear spindles with attached kinetochores, radiating from the nuclear poles within an intact nuclear membrane during schizogony, male gametogenesis, ookinete development and sporogony. Our data are consistent with a previous report, in which kinetochore localization was revealed using ultrastructural studies of *P. berghei* sporogony, and the duplication of half hemispindles during replication was suggested (Schrevel et al., 1977). Overall, based on all these results, consistent kinetochore clustering is present within Apicomplexa.

NDC80 is a major constituent of kinetochores and is highly conserved among eukaryotes including *Plasmodium.* However, many of the molecular details of kinetochore architecture and function in *Plasmodium* remain to be explored. A recent comparative evolutionary analysis suggested a distinct kinetochore network in many eukaryotes including *P. falciparum* and other Alveolates, with most of the highly conserved kinetochore complex proteins being absent in Plasmodium (van Hooff et al., 2017). Of 70 conserved kinetochore proteins only eleven are encoded in the *P. falciparum* genome. These eleven proteins include NDC80, NUF2, CENP(C/A/E), SPC25 and others that are highly conserved across 90 eukaryotic species, but genes for many other conserved proteins like SPC24, MAD(1/2) and MIS12 are absent (van Hooff et al., 2017). Recent studies have shown the presence of unconventional kinetochore

bioRxiv preprint doi: https://doi.org/10.1101/767830; this version posted September 26, 2019. The copyright holder for this preprint (which was not certified by peer review) is the author/funder. All rights reserved. No reuse allowed without permission.

proteins in kinetoplastids (Akiyoshi and Gull, 2014; D'Archivio and Wickstead, 2017), suggesting that different kinetochore architectures are possible. Therefore, it will be interesting to identify the NDC80 interacting partners and other potentially unconventional kinetochore proteins present in *Plasmodium* spp.

In summary, this study demonstrates the dynamic expression and location of NDC80 during the different proliferative stages of the malaria parasite and reveals the clustering of kinetochores and centromeres. It also shows the asynchronous closed mitotic division of *Plasmodium* during schizogony and sporogony, and provides new insights into the synchrony of chromosome replication in male gametogenesis and the first stages of meiosis in ookinetes. The transgenic parasite lines expressing NDC80 tagged with GFP and mCherry will be very useful resources for the *Plasmodium* community to facilitate future studies of cell division and comparative analyses of chromosome dynamics.

bioRxiv preprint doi: https://doi.org/10.1101/767830; this version posted September 26, 2019. The copyright holder for this preprint (which was not certified by peer review) is the author/funder. All rights reserved. No reuse allowed without permission.

Material and Methods:

Ethical statement

All animal-related work performed at the University of Nottingham has undergone an ethical review process and been approved by the United Kingdom Home Office with the project license number 30/3248. The work has been carried out in accordance with the United Kingdom 'Animals (Scientific Procedures) Act 1986' and was in compliance with 'European Directive 86/609/EEC' for the protection of animals used for experimental purposes. A combination of ketamine followed by antisedan was used for general anaesthesia and sodium pentobarbital was used for terminal anaesthesia. Proper care and efforts were made to minimise animal usage and suffering.

Six to eight-week-old female Tuck-Ordinary (TO) (Harlan) or CD1 outbred mice (Charles River) were used for all experiments.

Generation of transgenic parasites

The transgenic lines for NDC80 (PBANKA_1115700) were created using single homologous recombination as shown in **Fig. S1**. The oligonucleotides used to generate transgenic lines are provided in Supplementary Table S1. For GFP tagging, a 1153bp region of *ndc80* without the stop codon was inserted upstream of the *gfp* sequence in the p277 plasmid vector using KpnI and ApaI restriction sites as described previously (Tewari et al., 2010). The p277 vector contains the human *dhfr* cassette, conveying resistance to pyrimethamine. Before transfection, the sequence was linearised using EcoRV. The *P. berghei* ANKA line 2.34 was used for transfection by electroporation (Janse et al., 2006). Immediately, electroporated parasites were mixed with 100µl of reticulocyte-rich blood from a phenylhydrazine (6 mg/ml, Sigma) treated, naïve mouse and incubated at 37°C for 30 min before intraperitoneal injection. Pyrimethamine (70 mg/L, Sigma) was supplied in the drinking water from 1-day post-infection (dpi) to 4-dpi. Infected mice were monitored for 15 days and drug selection was repeated after passage to a second mouse. Integration PCR and western blot were performed to confirm successful generation of the transgenic line. For integration PCR, primer 1 (IntT259) and primer 2 (ol492) were used to confirm integration of the GFP targeting construct. Primer 1 and primer 3 (T2592) were used as a control. We also generated a mCherry-tagged NDC80 transgenic parasite line as shown in the schematic provided in **Fig. S1.**

Western Blot

bioRxiv preprint doi: https://doi.org/10.1101/767830; this version posted September 26, 2019. The copyright holder for this preprint (which was not certified by peer review) is the author/funder. All rights reserved. No reuse allowed without permission.

For western blotting, purified schizonts were lysed using lysis buffer (10 mM TrisHCl pH 7.5, 150 mM NaCl, 0.5 mM EDTA, 1% NP-40 and 1% Sarkosyl). The samples were boiled for 10 min after adding Laemmli sample buffer to the lysed cells. The sample was centrifuged at 13500 g for 5 min and electrophoresed on a 4–12% SDS-polyacrylamide gel. Subsequently, resolved proteins were transferred to nitrocellulose membrane (Amersham Biosciences) and immunoblotting was performed using the Western Breeze Chemiluminescence Anti-Rabbit kit (Invitrogen) and anti-GFP polyclonal antibody (Invitrogen) at a dilution of 1:1250, according to the manufacturer's instructions.

Localization of NDC80GFP throughout the parasite life cycle

Live cell imaging of transgenic parasite lines was performed at different proliferative stages during the parasite life cycle (Figure 1) as described previously (Roques et al., 2019; Saini et al., 2017) using a Zeiss AxioImager M2 microscope fitted with an AxioCam ICc1 digital camera (Carl Zeiss, Inc).

Blood stage schizogony

Infected mouse blood provided asexual blood and gametocyte stages of the *P. berghei* life cycle. Schizont culture (RPMI 1640 containing 25 mM HEPES, 1:10 (v/v) fetal bovine serum and penicillin/streptomycin 1:100) at different time points was used to analyse various stages of asexual development from ring to merozoite. The periods used for analysis and imaging werer 0 to1 h for ring stage parasites, 2 to 4 h for trophozoites, 6 to 8 h for early and mid-stage schizonts, 9 to 11 h for late segmented schizonts, and 18 to 24 h for mature schizonts and released merozoites in schizont culture medium.

Male gametocyte development

In vitro cultures were prepared to analyse non-activated gametocytes, activated gametocytes and male exflagellation. For *in vitro* exflagellation studies, gametocyte-infected blood was obtained from the tails of infected mice using a heparinised pipette tip. Gametocyte activation was performed by mixing 100µl of ookinete culture medium (RPMI 1640 containing 25 mM HEPES, 20% fetal bovine serum, 10 mM sodium bicarbonate, 50 µM xanthurenic acid at pH 7.6) with gametocyte-infected blood. To study different time points during microgametogenesis, gametocytes were purified using Nycodenz gradient (48%) and monitored at different time points to study mitotic division (male gametogenesis, 0 to 15 min post-activation (mpa).

Ookinete development

bioRxiv preprint doi: https://doi.org/10.1101/767830; this version posted September 26, 2019. The copyright holder for this preprint (which was not certified by peer review) is the author/funder. All rights reserved. No reuse allowed without permission.

To study ookinete development, gametocyte infected blood was incubated in ookinete medium for 24 hpa and various stages of zygote differentiation and ookinete development were monitored at different time points (0 min for nonactivated gametocytes, 30 min for activated gametocytes, 2 to 3 h for zygotes, 4 to 5 h for stage I, 5 to 6 h for stage II, 7 to 8 h for stage III, 8 to 10 h for stage IV, 11 to 14h for stage V, and 18 to 24 h for mature ookinetes post activation in ookinete medium).

Oocyst and sporozoite development

For mosquito transmission stages and bite back experiments, triplicate sets of 30 to 50 *Anopheles stephensi* mosquitoes were used. The mosquito guts were analysed on different days post-infection (dpi): 7 dpi, 12 dpi, 14 dpi and 21 dpi to check expression and localization of NDC80GFP during oocyst development and sporozoite formation.

Schizogony in liver stage

To study localization of NDC80-GFP in *P. berghei* liver stages, 100,000 HeLa cells were seeded in glass-bottomed imaging dishes. Salivary glands of female *A. stephensi* mosquitoes infected with NDC80-GFP parasites were isolated and sporozoites were released using a pestle to disrupt salivary gland cells. The released sporozoites were pipetted gently onto the HeLa cells and incubated at 37 °C in 5% CO_2 in air, in complete minimum Eagle's medium containing 2.5 µg/ml amphotericin B. For initial infection, medium was changed at 3 h post-infection and thereafter once a day. To perform live cell imaging, Hoechst 33342 (Molecular Probes) was added (1 µg/ml) and imaging was done at 55 h post-infection using a Leica TCS SP8 confocal microscope with the HC PL APO 63x/1.40 oil objective and the Leica Application Suite X software.

Indirect immunofluorescence assay

IFA studies were performed using poly-L-lysine coated slides on which schizonts had been previously fixed in 2% paraformaldehyde (PFA) in microtubule stabilising buffer (MTSB:10 mM MES, 150 mM NaCl, 5 mM EGTA, 5 mM $MgCl_2$, 5 mM glucose) in 1X-PBS for 30 min at room temperature (RT) and smeared onto slides. The fixed cells were permeablized using TBS containing 0.2% TritonX-100 for 5 min and washed three times with TBS before blocking. For blocking, 1hour incubation was performed with TBS solution containing 3% BSA (w/v) and 10% goat serum (v/v). TBS containing 1% BSA and 1% goat serum was used to dilute the antibodies for the incubations. Anti-GFP rabbit antibody (Invitrogen) was used at 1:250 dilution, anti-alpha-tubulin mouse antibody (Sigma-Aldrich) was used at 1:1000 dilution, and anti-centrin mouse clone 20h5 antibody (Millipore) was used at 1:200 dilution; each was

bioRxiv preprint doi: https://doi.org/10.1101/767830; this version posted September 26, 2019. The copyright holder for this preprint (which was not certified by peer review) is the author/funder. All rights reserved. No reuse allowed without permission.

incubated for 1 hour at RT. Three washes were performed with TBS, then AlexaFluor 568 labelled anti-rabbit (red) and AlexaFluor 488 labelled anti-mouse (green) (Invitrogen) (1:1000 dilution) were used as secondary antibodies and incubated for 40 min at RT. A similar protocol was followed for gametocytes except the cells were fixed in 4% PFA in MTSB. Slides were mounted with Vectashield containing DAPI (blue) and sealed using nail polish. Images were captured as described for live imaging.

Super resolution microscopy

A small volume (3 µl) of schizont culture was mixed with Hoechst dye and pipetted onto 2 % agarose pads (5x5 mm squares) at room temperature. After 3 min these agarose pads were placed onto glass bottom dishes with the cells facing towards glass surface (MatTek, P35G-1.5-20-C). Cells were scanned with an inverted microscope using Zeiss C-Apochromat 63×/1.2 W Korr M27 water immersion objective on a Zeiss Elyra PS.1 microscope, using the structured illumination microscopy (SIM) technique. The correction collar of the objective was set to 0.17 for optimum contrast. The following settings were used in SIM mode: lasers, 405 nm: 20%, 488 nm: 50%; exposure times 100 ms (Hoechst) and 25 ms (GFP); three grid rotations, five phases. The band pass filters BP 420-480 + LP 750 and BP 495-550 + LP 750 were used for the blue and green channels, respectively. Multiple focal planes (Z stacks) were recorded with 0.2 µm step size; later post-processing, a Z correction was done digitally on the 3D rendered images to reduce the effect of spherical aberration (reducing the elongated view in Z; a process previously tested with fluorescent beads). Images were processed and all focal planes were digitally merged into a single plane (Maximum intensity projection). The images recorded in multiple focal planes (Z-stack) were 3D rendered into virtual models and exported as images and movies (see supplementary material). Processing and export of images and videos were done by Zeiss Zen 2012 Black edition, Service Pack 5 and Zeiss Zen 2.1 Blue edition.

Electron microscopy

Samples for different mitotic stages of parasite development including schizonts (24 hours in culture), activated male gametocytes (8 min post-activation), infected mosquito guts (12 to 14 days post infection) and the meiotic stage from the mature ookinete (24hours post-activation) were fixed in 4% glutaraldehyde in 0.1 M phosphate buffer and processed for electron microscopy as previously described (Ferguson et al., 2005). Briefly, samples were post-fixed in osmium tetroxide, treated in bloc with uranyl acetate, dehydrated and embedded in Spurr's epoxy resin. Thin sections were stained with uranyl acetate and lead citrate prior to examination in a JEOL1200EX electron microscope (Jeol UK Ltd).

bioRxiv preprint doi: https://doi.org/10.1101/767830; this version posted September 26, 2019. The copyright holder for this preprint (which was not certified by peer review) is the author/funder. All rights reserved. No reuse allowed without permission.

Competing interests

The authors declare no competing interests.

Acknowledgements

We thank Prof. Snezhana Oliferenko, The Francis Crick Institute, for stimulating discussions and advice on kinetochore proteins. This project was funded by MRC project grants and MRC Investigators grants awarded to RT (G0900109, G0900278, MR/K011782/1) and BBSRC (BB/N017609/1). RP was supported by MRC grant MR/K011782/1. AAH was supported by the Francis Crick Institute (FC001097), which receives its core funding from Cancer Research UK (FC001097), the UK Medical Research Council (FC001097), and the Wellcome Trust (FC001097).

Author contribution

RT conceived and designed all experiments. RT, RP, MZ, ER and DB performed the experiments; RRS performed liver stage imaging; RP and RM performed super-resolution imaging; DJPF performed electron microscopy; RP, MZ, AAH, and RT analysed the data; RP, MZ, DSG, AAH and RT wrote the manuscript and all others contributed to it.

Funding

This project was funded by MRC project grant (MR/K011782/1) and BBSRC (BB/N017609/1) to RT. RP was supported by MRC grant MR/K011782/1. MZ was supported by BBSRC (BB/N017609/1). AAH was supported by the Francis Crick Institute, which receives its core funding from Cancer Research UK (FC001097), the UK Medical Research Council (FC001097), and the Wellcome Trust (FC001097).

Figure legends:

Fig. 1: Life cycle of rodent malaria parasite *Plasmodium berghei*. (**A)** represents endomitotic division: schizogony (schizont formation) in the liver and blood cells of the mammalian host and sporogony (sporozoite formation) in the mosquito gut. (**B)** and **(C)** represent atypical mitotic division by endoreduplication during male gametogenesis and meiotic division during the zygote to ookinete differentiation in the mosquito gut, respectively.

Fig. 2: NDC80-GFP localization during endomitotic cell division in schizogony. **(A)** Live cell imaging of NDC80GFP expression and location during asexual blood stage (DIC: Differential interference contrast, Hoechst: DNA, NDC80-GFP: GFP, Merge: Hoechst and GFP fluorescence, Troph: Trophozoite, Sch-E: Early Schizont, Sch-M: Mid Schizont Sch-L:

bioRxiv preprint doi: https://doi.org/10.1101/767830; this version posted September 26, 2019. The copyright holder for this preprint (which was not certified by peer review) is the author/funder. All rights reserved. No reuse allowed without permission.

Late Schizont, Mero: Merozoite, 100x magnification, Scale bar = 5 µM.) and schematic guide depicting NDC80 localization during various developmental stages in the bloodstream of the parasite life cycle. **(B)** Live cell super-resolution 3D imaging for NDC80-GFP localization during asynchronous blood stage mitotic division. Scale bar = 5 µM. (**C)** Electron microscopy imaging of an early schizont showing kinetochore localization. **(i)** Section through an early schizont within a red blood cell, showing two nuclei (N) and the food vacuole (FV). Scale bar = 1 µm. **(ii)** Enlargement of the enclosed area showing part of the nucleus in which a nuclear pole (NP), microtubules and attached kinetochores (K) can be seen. Scale bar = 100 nm. (**D-E**) Immunofluorescence fixed cell imaging and schematic guide of NDC80-GFP and co-localization with antibodies specific for α-tubulin (**D**) and centrin (**E**) in mitotic cells (100x magnification). Scale bar = 5 µM.

Fig. 3: Temporal dynamics of NDC80-GFP during male gametogenesis. (A) Live cell imaging for NDC80-GFP expression and location during endoreduplicative mitotic division in male gametogenesis (100x magnification) and a schematic representation at the different time points. **(B-C)** Time-lapse screenshots for NDC80-GFP localization during male gametogenesis. Scale bar = 5 µM. (**D)** Electron microscopy on 8 min post-activation gametocytes for kinetochore localization. **(i)** Section through a mid-stage microgametocyte showing the large central nucleus (N) with axonemes (A) present in the peripheral cytoplasm. Scale bar = 1 µm. (**ii)** Enlargement of the enclosed area showing the details of a nuclear spindle with microtubules with attach kinetochores (K) radiating from the nuclear poles (NP). Scale bar = 100nm.

Fig. 4: Spatiotemporal profile of NDC80-GFP expression during meiotic stages in the ookinete. (**A**) Live cell imaging of NDC80-GFP localization during various stage of ookinete development from zygote to mature ookinete in the mosquito gut (100x magnification). Merge: Hoechst (blue, DNA), GFP (green) and P28 (red, cell surface marker of activated female gamete, zygote and ookinete stages). Scale bar = 5 µM. (**B**) Ultrastructural analysis of kinetochore localization in a mature ookinete. (**i**) Longitudinal section through a mature ookinete showing the apical complex with several micronemes (M) and the more posterior nucleus (N). Scale bar = 1 µm. (**ii)** Enlargement of the nucleus showing the location of the four nuclear poles (arrows). Scale bar = 100 nm.

Fig. 5: NDC80-GFP localisation during oocyst development and sporozoite formation. (**A**) Live cell imaging of NDC80-GFP in oocysts at 7, 12, 14 and 21 days post-infection (dpi) and a sporozoite. Panels: DIC (differential interference contrast), Hoechst (blue, DNA), NDC80GFP (green, GFP), Merged: Hoechst (blue, DNA) and NDC80-GFP (green, GFP) Scale bar = 5µM. **(B)** Electron microscopy analysis of kinetochore location in an oocyst 12 day

bioRxiv preprint doi: https://doi.org/10.1101/767830; this version posted September 26, 2019. The copyright holder for this preprint (which was not certified by peer review) is the author/funder. All rights reserved. No reuse allowed without permission.

post-infection. **(i)** Central section through a mid-stage oocyst showing the early stages of sporozoite formation (S) at the surface of the oocyst cytoplasm. Scale bar = 10 µm. **(ii)** Detail showing the early stage in sporozoite budding. Note the underlying nucleus (N) with the nuclear pole and attached kinetochores (K) directed toward the budding sporozoite. R – Rhoptry anlagen. Scale bar = 100 nm.

Fig. S1:- Generation and genotype analysis of NDC80-GFP/mCherry parasite line. (A) Schematic representation of the endogenous *ndc80*, the GFP/mCherry-tagging construct and the recombined *ndc80* locus following single homologous recombination. Arrows 1, 2 and 3 indicate the position of PCR primers used to confirm successful integration of the construct. (B) Diagnostic PCR of NDC80-GFP and WTGFP parasites using primers IntT259 (NDC80, Arrow 1) and ol492 (for GFP line)/mCherry (for mCherry) (Arrow 3). IntT259 and T2592 (NDC80, Arrow 2) primers were used as control. Integration of the NDC80 tagging construct gives a band of 1269bp (GFP line) and 1335bp (mCherry line) for NDC80 parasite line. For controls, both WT and NDC80 tagged constructs gave a band size of 1153 bp. (C) Western blot of NDC80-GFP (96 kDa) and WTGFP (29kDa) protein to illustrate the presence of intact NDC80-GFP in schizont stage extracts.

Fig. S2: Expression and location of NDC80-mCherry in asexual blood stages. Fluorescence was detected by live cell imaging. DIC: Differential interference contrast; Hoechst: blue, DNA; mCherry: red, NDC80-mCherry; Merge: Hoechst and mCherry fluorescence. Scale bar = 5µM.

Fig. S3: Localization of *Plasmodium* NDC80-GFP in liver stage. Expression of the protein was detected in liver schizonts by live cell imaging. Merge = DAPI and GFP. Scale bar = 5 µM.

Fig. S4: Expression and location of NDC80-GFP in gametocytes and gametes. Non-activated and activated gametocytes and gametes were examined by live cell imaging (100x magnification). DIC: differential interference contrast; Hoechst (blue, DNA), NDC80-GFP (green, GFP); P28 (red, cell surface marker of activated female gamete); Merge: Hoechst (blue, DNA), GFP (green) and P28 (red).

Supplementary Table S1: Primers used in this study

Supplementary Videos

SV1, SV2 and SV3: Three-dimensional rendered 3 (SIM Structure Illumination) of NDC80-GFP with respect to DAPI-stained nuclear DNA during schizogony.

bioRxiv preprint doi: https://doi.org/10.1101/767830; this version posted September 26, 2019. The copyright holder for this preprint (which was not certified by peer review) is the author/funder. All rights reserved. No reuse allowed without permission.

SV4: Time lapse video showing dynamics of NDC80-GFP during gametogony in 0-70 seconds

SV5: Time lapse video showing dynamics of NDC80-GFP during gametogony in 90-160 seconds

References

Akiyoshi, B., and K. Gull. 2013. Evolutionary cell biology of chromosome segregation: insights from trypanosomes. *Open biology*. 3:130023.

Akiyoshi, B., and K. Gull. 2014. Discovery of unconventional kinetochores in kinetoplastids. *Cell*. 156:1247-1258.

Alushin, G.M., V.H. Ramey, S. Pasqualato, D.A. Ball, N. Grigorieff, A. Musacchio, and E. Nogales. 2010. The Ndc80 kinetochore complex forms oligomeric arrays along microtubules. *Nature*. 467:805-810.

Arnot, D.E., and K. Gull. 1998. The Plasmodium cell-cycle: facts and questions. *Annals of tropical medicine and parasitology*. 92:361-365.

Arnot, D.E., E. Ronander, and D.C. Bengtsson. 2011. The progression of the intra-erythrocytic cell cycle of Plasmodium falciparum and the role of the centriolar plaques in asynchronous mitotic division during schizogony. *International journal for parasitology*. 41:71-80.

Biggins, S., and C.E. Walczak. 2003. Captivating capture: how microtubules attach to kinetochores. *Current biology : CB*. 13:R449-460.

Cheeseman, I.M. 2014. The kinetochore. *Cold Spring Harbor perspectives in biology*. 6:a015826.

Ciferri, C., J. De Luca, S. Monzani, K.J. Ferrari, D. Ristic, C. Wyman, H. Stark, J. Kilmartin, E.D. Salmon, and A. Musacchio. 2005. Architecture of the human ndc80-hec1 complex, a critical constituent of the outer kinetochore. *The Journal of biological chemistry*. 280:29088-29095.

D'Archivio, S., and B. Wickstead. 2017. Trypanosome outer kinetochore proteins suggest conservation of chromosome segregation machinery across eukaryotes. *The Journal of cell biology*. 216:379-391.

DeLuca, J.G., B. Moree, J.M. Hickey, J.V. Kilmartin, and E.D. Salmon. 2002. hNuf2 inhibition blocks stable kinetochore-microtubule attachment and induces mitotic cell death in HeLa cells. *The Journal of cell biology*. 159:549-555.

Doerig, C., D. Chakrabarti, B. Kappes, and K. Matthews. 2000. The cell cycle in protozoan parasites. *Prog Cell Cycle Res*. 4:163-183.

Drechsler, H., and A.D. McAinsh. 2012. Exotic mitotic mechanisms. *Open biology*. 2:120140.

bioRxiv preprint doi: https://doi.org/10.1101/767830; this version posted September 26, 2019. The copyright holder for this preprint (which was not certified by peer review) is the author/funder. All rights reserved. No reuse allowed without permission.

Farrell, M., and M.J. Gubbels. 2014. The Toxoplasma gondii kinetochore is required for centrosome association with the centrocone (spindle pole). *Cellular microbiology*. 16:78-94.

Fennell, B.J., Z.A. Al-shatr, and A. Bell. 2008. Isotype expression, post-translational modification and stage-dependent production of tubulins in erythrocytic Plasmodium falciparum. *International journal for parasitology*. 38:527-539.

Ferguson, D.J., A.E. Balaban, E.M. Patzewitz, R.J. Wall, C.S. Hopp, B. Poulin, A. Mohmmed, P. Malhotra, A. Coppi, P. Sinnis, and R. Tewari. 2014. The repeat region of the circumsporozoite protein is critical for sporozoite formation and maturation in Plasmodium. *PloS one*. 9:e113923.

Ferguson, D.J., F.L. Henriquez, M.J. Kirisits, S.P. Muench, S.T. Prigge, D.W. Rice, C.W. Roberts, and R.L. McLeod. 2005. Maternal inheritance and stage-specific variation of the apicoplast in Toxoplasma gondii during development in the intermediate and definitive host. *Eukaryotic cell*. 4:814-826.

Ferguson, D.J.P., N. Sahoo, R.A. Pinches, J.M. Bumstead, F.M. Tomley, and M.-J. Gubbels. 2008. MORN1 has a conserved role in asexual and sexual development across the apicomplexa. *Eukaryotic cell*. 7:698-711.

Francia, M.E., J.F. Dubremetz, and N.S. Morrissette. 2015. Basal body structure and composition in the apicomplexans Toxoplasma and Plasmodium. *Cilia*. 5:3.

Francia, M.E., and B. Striepen. 2014. Cell division in apicomplexan parasites. *Nature reviews. Microbiology*. 12:125-136.

Gerald, N., B. Mahajan, and S. Kumar. 2011. Mitosis in the human malaria parasite Plasmodium falciparum. *Eukaryotic cell*. 10:474-482.

Guttery, D.S., M. Roques, A.A. Holder, and R. Tewari. 2015. Commit and Transmit: Molecular Players in Plasmodium Sexual Development and Zygote Differentiation. *Trends Parasitol*. 31:676-685.

Hoeijmakers, W.A., C. Flueck, K.J. Francoijs, A.H. Smits, J. Wetzel, J.C. Volz, A.F. Cowman, T. Voss, H.G. Stunnenberg, and R. Bartfai. 2012. Plasmodium falciparum centromeres display a unique epigenetic makeup and cluster prior to and during schizogony. *Cellular microbiology*. 14:1391-1401.

Iwanaga, S., S.M. Khan, I. Kaneko, Z. Christodoulou, C. Newbold, M. Yuda, C.J. Janse, and A.P. Waters. 2010. Functional identification of the Plasmodium centromere and generation of a Plasmodium artificial chromosome. *Cell host & microbe*. 7:245-255.

Janse, C.J., B. Franke-Fayard, G.R. Mair, J. Ramesar, C. Thiel, S. Engelmann, K. Matuschewski, G.J. van Gemert, R.W. Sauerwein, and A.P. Waters. 2006. High efficiency transfection of Plasmodium berghei facilitates novel selection procedures. *Molecular and biochemical parasitology*. 145:60-70.

bioRxiv preprint doi: https://doi.org/10.1101/767830; this version posted September 26, 2019. The copyright holder for this preprint (which was not certified by peer review) is the author/funder. All rights reserved. No reuse allowed without permission.

Janse, C.J., T. Ponnudurai, A.H. Lensen, J.H. Meuwissen, J. Ramesar, M. Van der Ploeg, and J.P. Overdulve. 1988. DNA synthesis in gametocytes of Plasmodium falciparum. *Parasitology*. 96 (Pt 1):1-7.

McKinley, K.L., and I.M. Cheeseman. 2016. The molecular basis for centromere identity and function. *Nature reviews. Molecular cell biology*. 17:16-29.

Musacchio, A., and A. Desai. 2017. A Molecular View of Kinetochore Assembly and Function. *Biology*. 6.

Petrovic, A., J. Keller, Y. Liu, K. Overlack, J. John, Y.N. Dimitrova, S. Jenni, S. van Gerwen, P. Stege, S. Wohlgemuth, P. Rombaut, F. Herzog, S.C. Harrison, I.R. Vetter, and A. Musacchio. 2016. Structure of the MIS12 Complex and Molecular Basis of Its Interaction with CENP-C at Human Kinetochores. *Cell*. 167:1028-1040 e1015.

Richmond, D., R. Rizkallah, F. Liang, M.M. Hurt, and Y. Wang. 2013. Slk19 clusters kinetochores and facilitates chromosome bipolar attachment. *Molecular biology of the cell*. 24:566-577.

Roques, M., R.R. Stanway, E.I. Rea, R. Markus, D. Brady, A.A. Holder, D.S. Guttery, and R. Tewari. 2019. Plasmodium centrin PbCEN-4 localizes to the putative MTOC and is dispensable for malaria parasite proliferation. *Biology open*. 8.

Saini, E., M. Zeeshan, D. Brady, R. Pandey, G. Kaiser, L. Koreny, P. Kumar, V. Thakur, S. Tatiya, N.J. Katris, R.S. Limenitakis, I. Kaur, J.L. Green, A.R. Bottrill, D.S. Guttery, R.F. Waller, V. Heussler, A.A. Holder, A. Mohmmed, P. Malhotra, and R. Tewari. 2017. Photosensitized INA-Labelled protein 1 (PhIL1) is novel component of the inner membrane complex and is required for Plasmodium parasite development. *Scientific reports*. 7:15577.

Schrevel, J., G. Asfaux-Foucher, and J.M. Bafort. 1977. [Ultrastructural study of multiple mitoses during sporogony of Plasmodium b. berghei]. *Journal of ultrastructure research*. 59:332-350.

Sinden, R.E. 1983. Sexual development of malarial parasites. *Advances in parasitology*. 22:153-216.

Sinden, R.E. 1991a. Asexual blood stages of malaria modulate gametocyte infectivity to the mosquito vector--possible implications for control strategies. *Parasitology*. 103 Pt 2:191-196.

Sinden, R.E. 1991b. Mitosis and meiosis in malarial parasites. *Acta Leidensia*. 60:19-27.

Sinden, R.E., E.U. Canning, R.S. Bray, and M.E. Smalley. 1978. Gametocyte and gamete development in Plasmodium falciparum. *Proceedings of the Royal Society of London. Series B, Biological sciences*. 201:375-399.

bioRxiv preprint doi: https://doi.org/10.1101/767830; this version posted September 26, 2019. The copyright holder for this preprint (which was not certified by peer review) is the author/funder. All rights reserved. No reuse allowed without permission.

Sinden, R.E., E.U. Canning, and B. Spain. 1976. Gametogenesis and fertilization in Plasmodium yoelii nigeriensis: a transmission electron microscope study. *Proceedings of the Royal Society of London. Series B, Biological sciences*. 193:55-76.

Sinden, R.E., A. Talman, S.R. Marques, M.N. Wass, and M.J. Sternberg. 2010. The flagellum in malarial parasites. *Current opinion in microbiology*. 13:491-500.

Solovei, I., L. Schermelleh, K. During, A. Engelhardt, S. Stein, C. Cremer, and T. Cremer. 2004. Differences in centromere positioning of cycling and postmitotic human cell types. *Chromosoma*. 112:410-423.

Sundin, L.J., G.J. Guimaraes, and J.G. Deluca. 2011. The NDC80 complex proteins Nuf2 and Hec1 make distinct contributions to kinetochore-microtubule attachment in mitosis. *Molecular biology of the cell*. 22:759-768.

Suvorova, E.S., M. Francia, B. Striepen, and M.W. White. 2015. A novel bipartite centrosome coordinates the apicomplexan cell cycle. *PLoS biology*. 13:e1002093.

Swedlow, J.R., K. Hu, P.D. Andrews, D.S. Roos, and J.M. Murray. 2002. Measuring tubulin content in Toxoplasma gondii: a comparison of laser-scanning confocal and wide-field fluorescence microscopy. *Proceedings of the National Academy of Sciences of the United States of America*. 99:2014-2019.

Tewari, R., D. Dorin, R. Moon, C. Doerig, and O. Billker. 2005. An atypical mitogen-activated protein kinase controls cytokinesis and flagellar motility during male gamete formation in a malaria parasite. *Molecular microbiology*. 58:1253-1263.

Tewari, R., U. Straschil, A. Bateman, U. Bohme, I. Cherevach, P. Gong, A. Pain, and O. Billker. 2010. The systematic functional analysis of Plasmodium protein kinases identifies essential regulators of mosquito transmission. *Cell host & microbe*. 8:377-387.

Vader, G., and A. Musacchio. 2017. The greatest kinetochore show on earth. *EMBO reports*. 18:1473-1475.

Vaishnava, S., D.P. Morrison, R.Y. Gaji, J.M. Murray, R. Entzeroth, D.K. Howe, and B. Striepen. 2005. Plastid segregation and cell division in the apicomplexan parasite Sarcocystis neurona. *Journal of cell science*. 118:3397-3407.

van Hooff, J.J., E. Tromer, L.M. van Wijk, B. Snel, and G.J. Kops. 2017. Evolutionary dynamics of the kinetochore network in eukaryotes as revealed by comparative genomics. *EMBO reports*. 18:1559-1571.

Wei, R.R., P.K. Sorger, and S.C. Harrison. 2005. Molecular organization of the Ndc80 complex, an essential kinetochore component. *Proceedings of the National Academy of Sciences of the United States of America*. 102:5363-5367.

Westermann, S., D.G. Drubin, and G. Barnes. 2007. Structures and functions of yeast kinetochore complexes. *Annual review of biochemistry*. 76:563-591.

WHO. 2018. World malaria report 2018. *World Health Organization*.

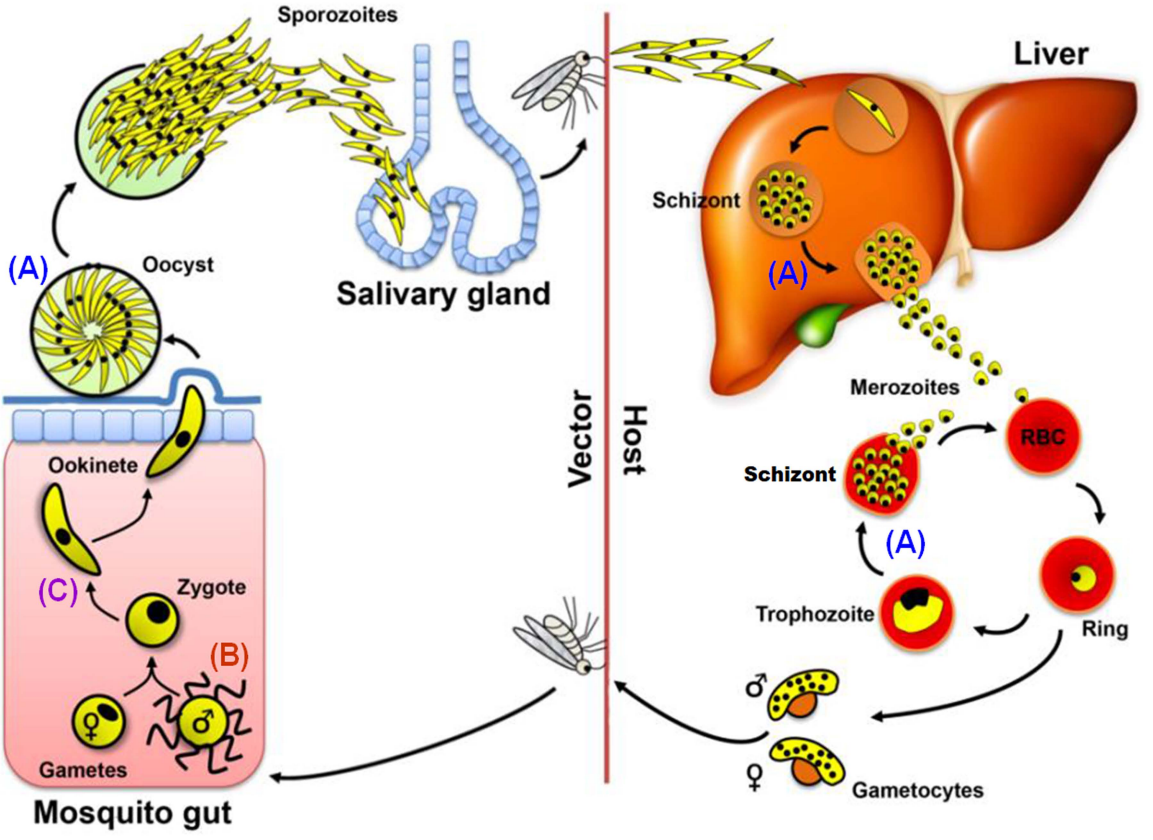

A- Endomitotic division (Schizogony- schizont formation in the mammalian liver and blood cells and sporogony (sporozoite formation) in the mosquito gut. B- endoreduplication (Male gametogenesis in mosquito gut). C- Meiotic cell division (zygote to ookinete differentiation in the mosquito gut)

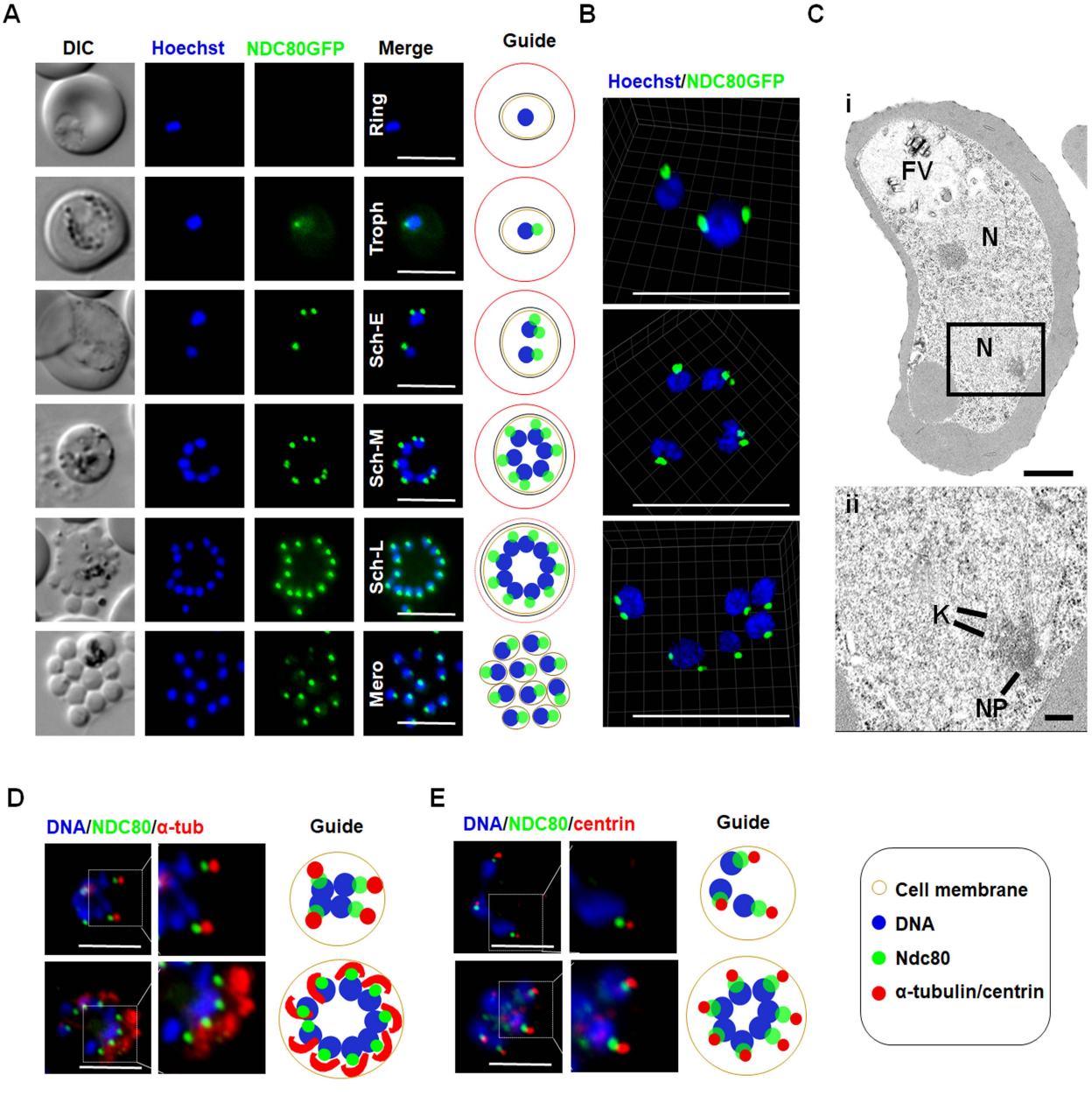
A
DIC
Hoechst
NDC80GFP
Merge
Guide
Ring
Troph
Sch-E
Sch-M
Sch-L
Mero
B
Hoechst/NDC80GFP
C
i
FV
N
N
ii
K
NP
D
DNA/NDC80/α-tub
Guide
E
DNA/NDC80/centrin
Guide
Cell membrane
DNA
Ndc80
α-tubulin/centrin

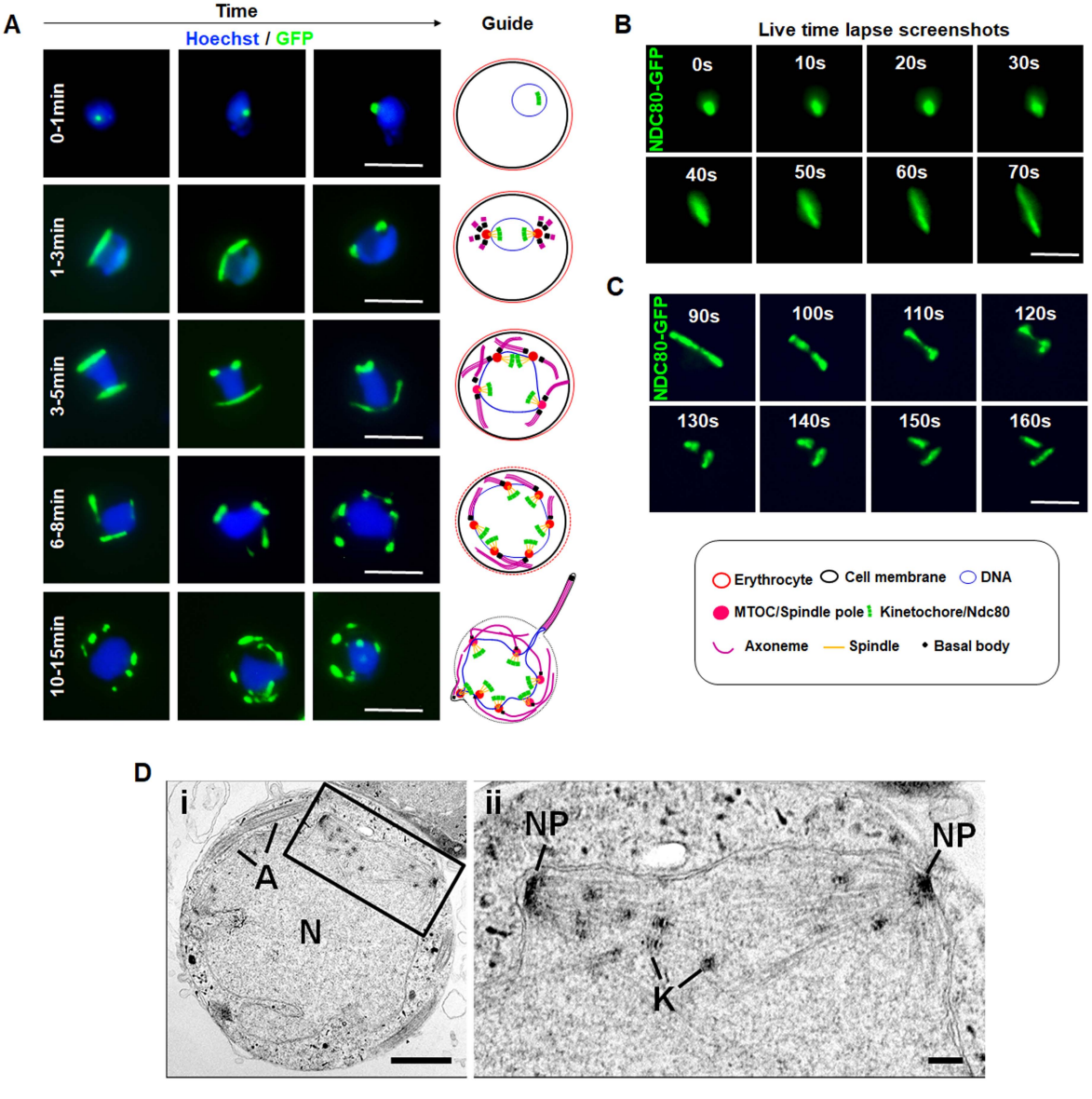
A
Time
Hoechst / GFP
Guide
0-1min
1-3min
3-5min
6-8min
10-15min
B
Live time lapse screenshots
NDC80-GFP
0s
10s
20s
30s
40s
50s
60s
70s
C
NDC80-GFP
90s
100s
110s
120s
130s
140s
150s
160s
Erythrocyte
Cell membrane
DNA
MTOC/Spindle pole
Kinetochore/Ndc80
Axoneme
Spindle
Basal body
D
i
A
N
ii
NP
NP
K

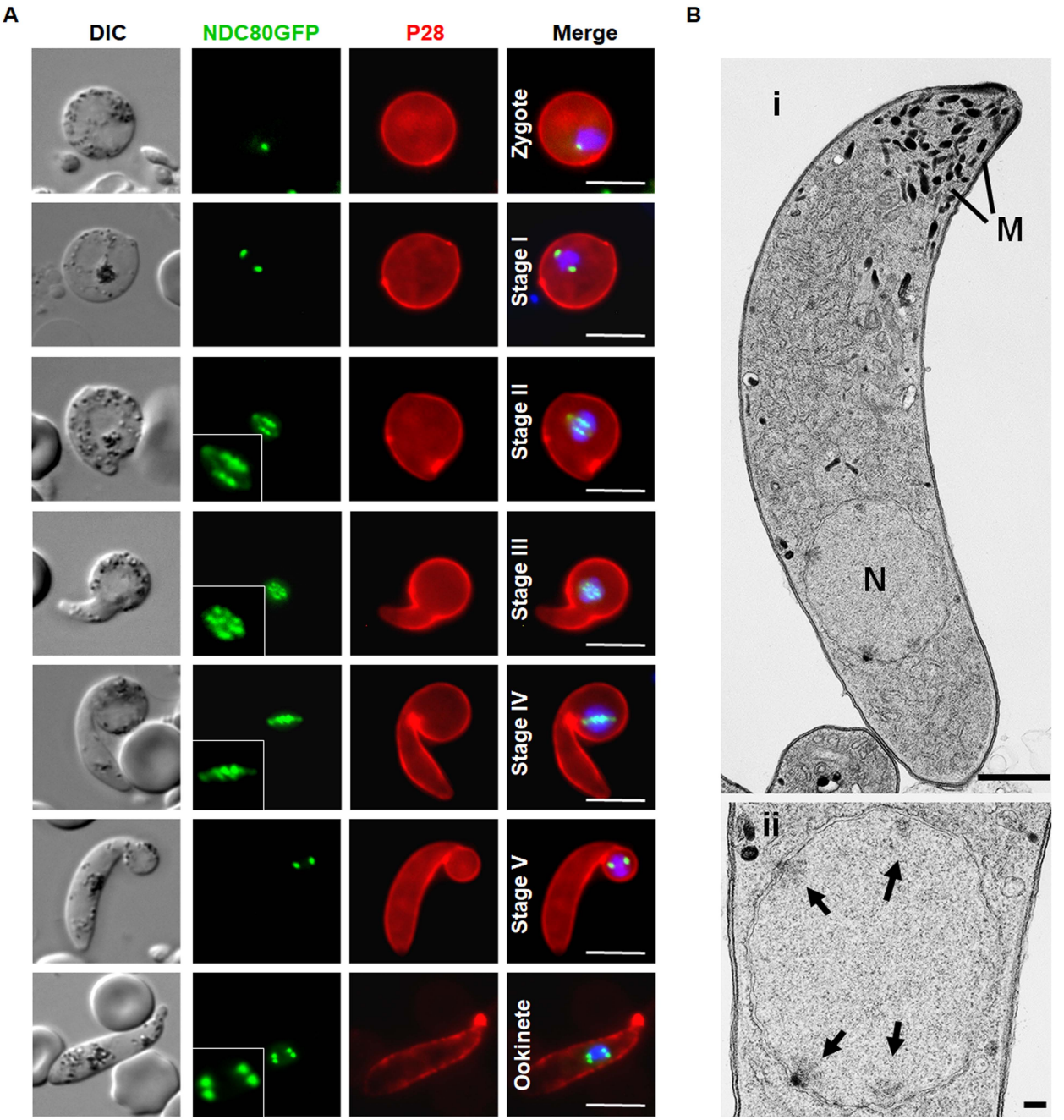
A
DIC
NDC80GFP
P28
Merge
Zygote
Stage I
Stage II
Stage III
Stage IV
Stage V
Ookinete
B
i
M
N
ii

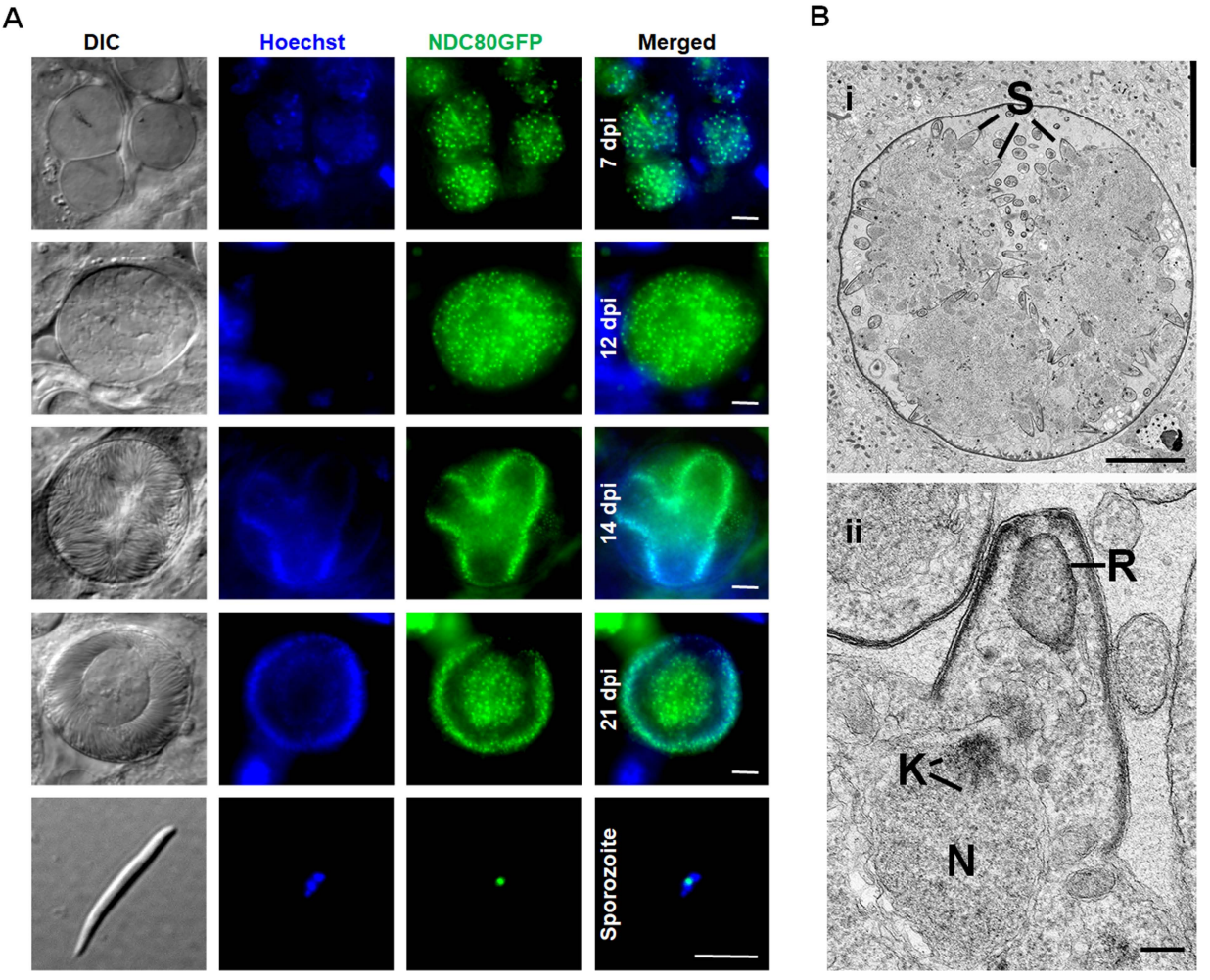
A
DIC
Hoechst
NDC80GFP
Merged
7 dpi
12 dpi
14 dpi
21 dpi
Sporozoite
B
i
S
ii
R
K
N

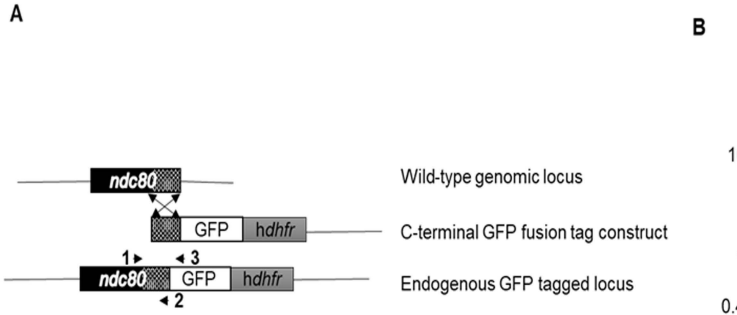
A
ndc80
Wild-type genomic locus
GFP
hdhfr
C-terminal GFP fusion tag construct
1
3
ndc80
GFP
hdhfr
Endogenous GFP tagged locus
2
ndc80
Wild-type genomic locus
mCherry
hdhfr
C-terminal mCherry fusion tag construct
1
3
ndc80
mCherry
hdhfr
Endogenous mCherry tagged locus
2

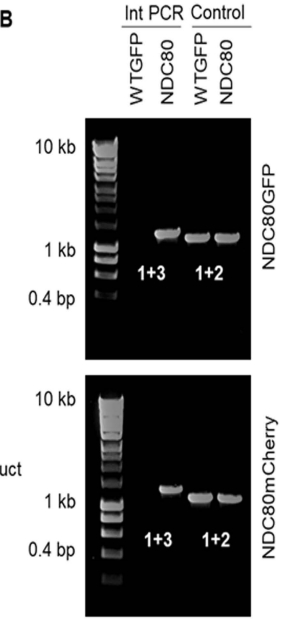
B
Int PCR Control
WTGFP
NDC80
WTGFP
NDC80
10 kb
1 kb
0.4 bp
1+3
1+2
NDC80GFP
10 kb
1 kb
0.4 bp
1+3
1+2
NDC80mCherry

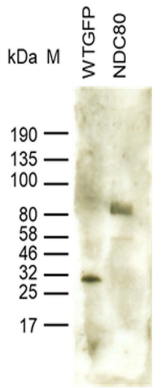
C
kDa M
WTGFP
NDC80
190
135
100
80
58
46
32
25
17

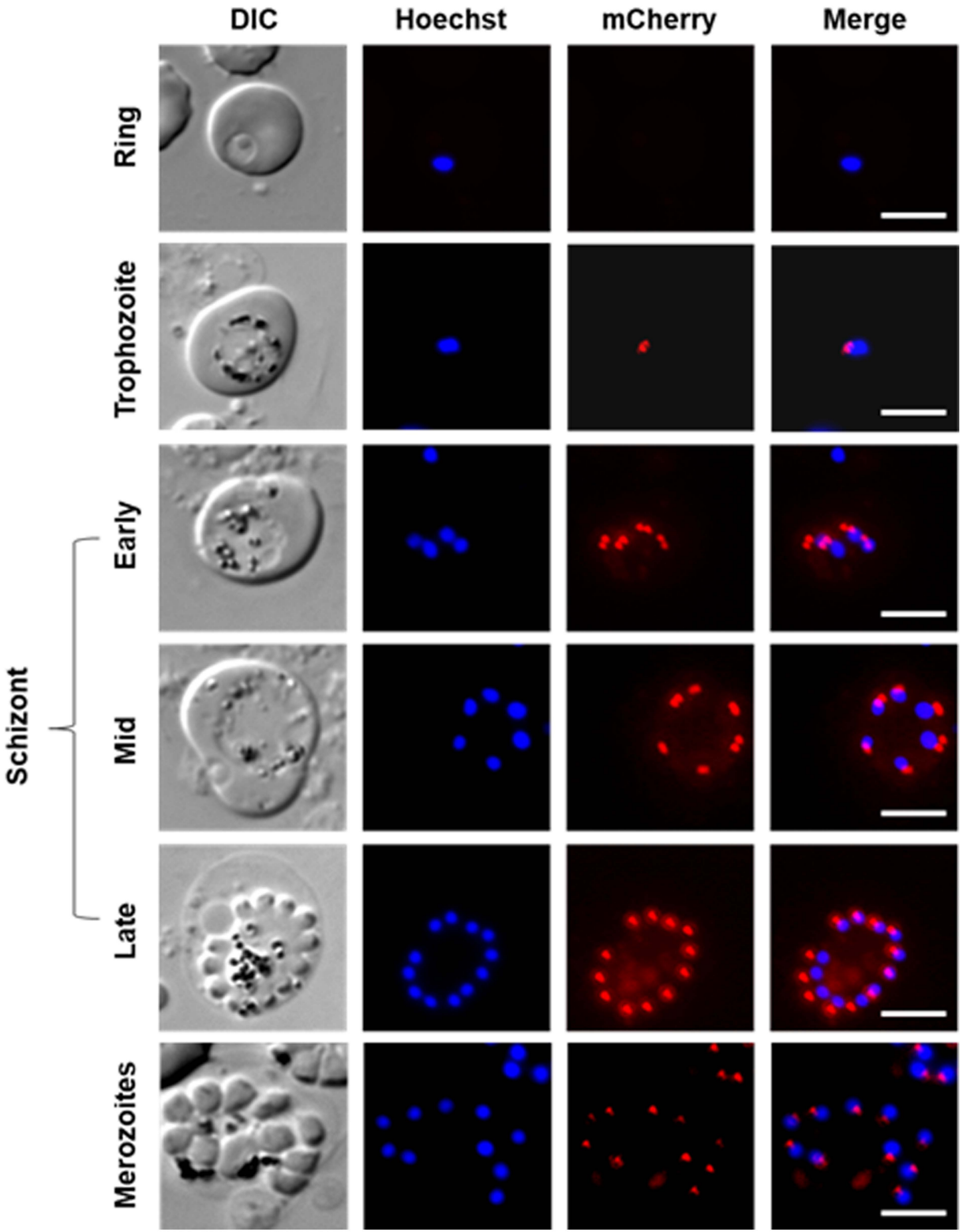
DIC
Hoechst
mCherry
Merge
Ring
Trophozoite
Early
Mid
Late
Schizont
Merozoites

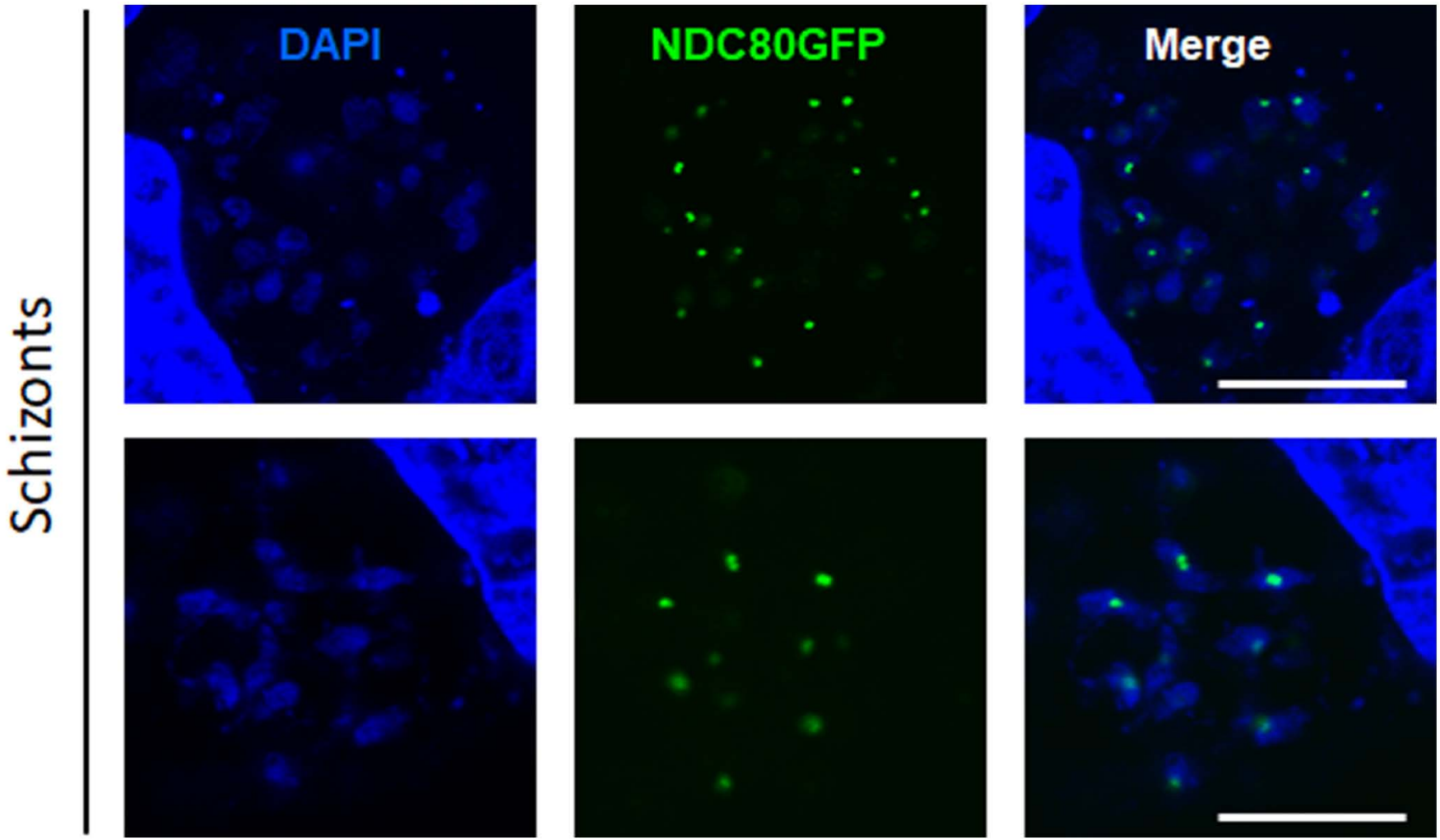
Schizonts
DAPI
NDC80GFP
Merge

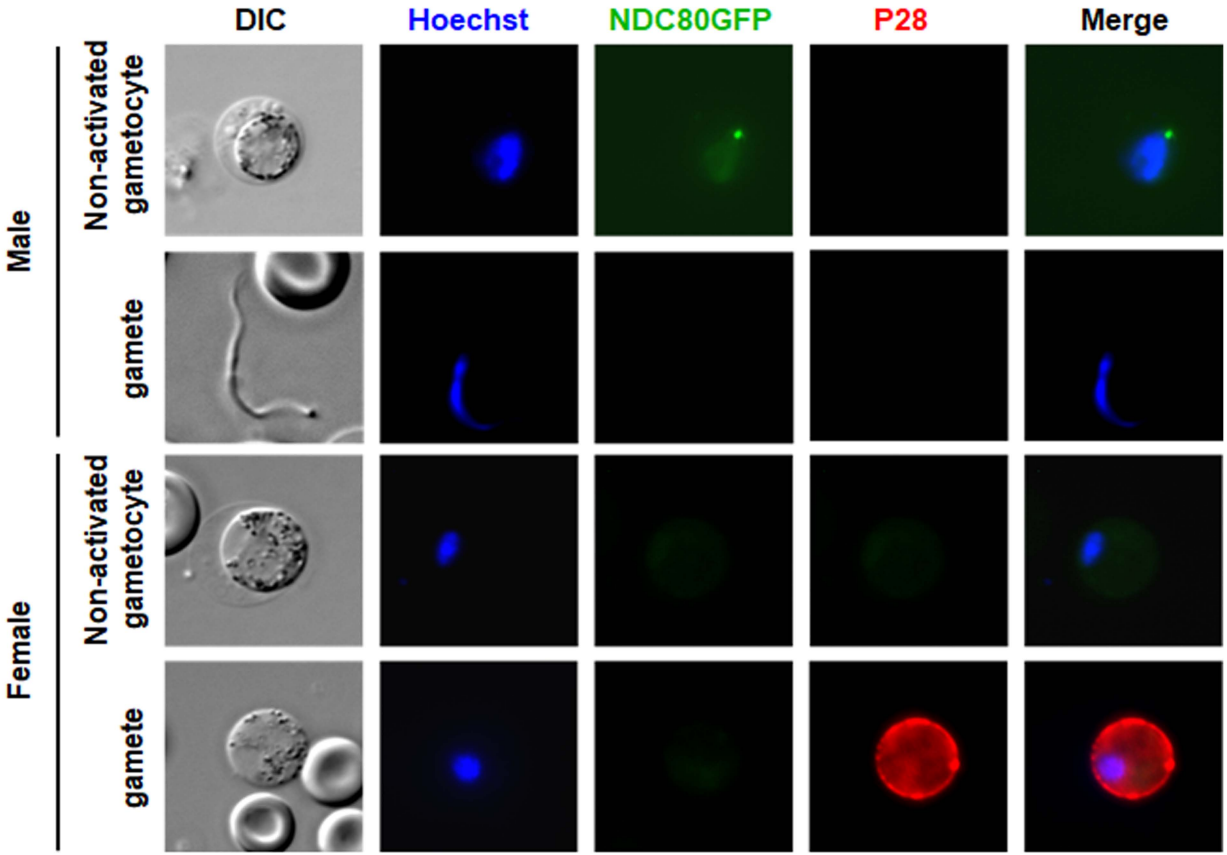
DIC
Hoechst
NDC80GFP
P28
Merge
Male
Non-activated gametocyte
gamete
Female
Non-activated gametocyte
gamete